CLEO RESULTS ON CHARM LEPTONIC AND SEMILEPTONIC DECAYS

S. STONE
Department of Physics, Syracuse University,
Syracuse, NY, 13244, USA

1 Introduction

Here I will review a small selection of recent CLEO results on purely leptonic and semileptonic decays mostly of the D_s^+ meson. In leptonic decays the quark and antiquark in the meson annihilate via a virtual W that materializes as a lepton (ℓ) anti-neutrino pair. To lowest order, the decay width is given by

$$\Gamma(P \to \ell\nu) = \frac{G_F^2}{8\pi} f_P^2 \, m_\ell^2 M_P \left(1 - \frac{m_\ell^2}{M_P^2}\right)^2 \left|V_{q_1 q_2}\right|^2 \ , \tag{1}$$

where M_P is the P mass, m_ℓ is the ℓ mass, $V_{q_1 q_2}$ is the Cabibbo-Kobayashi-Maskawa (CKM) matrix element between the constituent quarks $q_1\bar{q}_2$ in P, and G_F is the Fermi coupling constant. The parameter f_P is the decay constant, the quantity to be measured or calculated, that is related to the wave-function overlap of the quark and antiquark.

2 Leptonic Decays

Near 4.170 GeV in center-of-mass energy e^+e^- collisions produce $D_s D_s^*$ pairs with about a 1 nb cross-section. The presence of the $D_s^* \to \gamma D_s$ transition makes the analysis of D_s^+ decays somewhat more complicated than studies at 3.770 GeV where D^+D^- and $D^0\overline{D^0}$ pairs are produced.

To study D^+ decays we fully reconstruct a D^- and then we use the conservation of energy and momentum to infer the presence of a missing neutrino in $D^+ \to \ell^+\nu$ (leptonic) or $D^+ \to h\ell^+\nu$ (semileptonic) decays. This is done by calculating the missing mass squared as

$$\mathrm{MM}^2 = \left(E_{\rm beam} - E_{\mu^+}\right)^2 - \left(-\mathbf{p}_{D^-} - \mathbf{p}_{\mu^+}\right)^2 , \tag{2}$$

here $E_{\rm beam}$ is the beam energy, $\mathbf{p}_{D^-}$ is the three-momentum of the fully reconstructed D^-, and $E_{\mu^+}(\mathbf{p}_{\mu^+})$ is the energy (momentum) of the μ^+ candidate. MM^2 peaks at zero for a missing ν.

To reconstruct D^- tags we require that the tag candidates have a measured energy consistent with the beam energy, and have a "beam constrained mass," m_{BC}, consistent with the D^- mass, where $m_{\rm BC} = \sqrt{E_{\rm beam}^2 - (\sum_i \mathbf{p}_i)^2}$, and i runs over all the final state particles three-momenta.

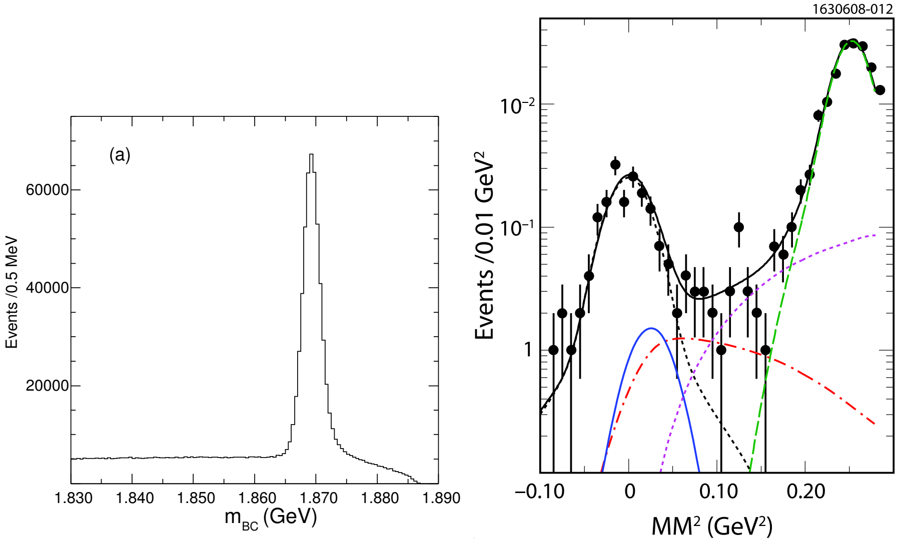

Figure 1: (a) The beam-constrained mass distributions summed over D^- decay candidates in the final states: $K^+\pi^-\pi^-$, $K^+\pi^-\pi^-\pi^0$, $K_s\pi^-$, $K_s\pi^-\pi^-\pi^+$, $K_s\pi^-\pi^0$ and $K^+K^-\pi^-$. (b) Fit to the MM^2. Data are points with error bars. The black (dashed) curve centered at zero shows the signal $\mu^+\nu$ events. The dot-dashed (red) curve that peaks around 0.05 GeV^2 shows $D^+ \to \tau^+\nu$, $\tau^+ \to \pi^+\bar{\nu}$. The solid (blue) Gaussian shaped curve centered on the pion-mass squared shows residual $\pi^+\pi^0$. The dashed (purple) curve that falls to zero around 0.03 GeV^2 is the sum of all the other background components, except the $\overline{K}^0\pi^+$ tail which is shown by the long-dashed (green) curve that peaks up at 0.25 GeV^2. The solid (black) curve is the sum of all the components.

Fig. 1(a) shows the m_{BC} distribution summed over all the decay modes we use for tagging. There are 460,055$\pm$787 plus 89,472 backgrounds. The fit to the MM^2 distribution shown in Fig. 1(b) contains separate shapes for signal, $\pi^+\pi^0$, $\overline{K}^0\pi^+$, $\tau^+\nu$ ($\tau^+ \to \pi^+\bar{\nu}$), and a background shape describing three-body decays. Here we constrain the ratio of the $\tau^+\nu/\mu^+\nu$ components to the SM ratio of 2.65. We also veto events with an extra neutral energy cluster $>$ 250 MeV which removes most $\pi^+\pi^0$ events. The normalizations of the signal, $\overline{K}^0\pi^+$, and 3-body background shapes are allowed to float. The final result, including radiative corrections is [1]

$$f_{D^+} = (206.7 \pm 8.5 \pm 2.5)\ \mathrm{MeV}\ . \tag{3}$$

For D_s^+ studies we first cut on the the invariant mass of the decay products of D_s^- tag candidates shown in Fig. 2(a), then detect an additional photon candidate from the D_s^* decay, and construct

$$\mathrm{MM}^{*2} = (E_{\mathrm{CM}} - E_{D_s} - E_\gamma)^2 - (\mathbf{p}_{\mathrm{CM}} - \mathbf{p}_{D_s} - \mathbf{p}_\gamma)^2\,, \tag{4}$$

where E_{CM} ($\mathbf{p}_{\mathrm{CM}}$) is the center-of-mass energy (momentum), E_{D_s} ($\mathbf{p}_{D_s}$) is the energy (momentum) of the fully reconstructed D_s^- tag, and E_γ ($\mathbf{p}_\gamma$) is the energy (momentum) of the additional photon. In performing this calculation we use a kinematic fit that constrains the decay products of the D_s^- to the known D_s mass and conserves overall momentum and energy. All photon candidates in the event are tried, except for those that are decay products of the D_s^- tag candidate. Regardless of whether or not the photon forms a D_s^* with the tag, for real $D_s^*D_s$ events the missing mass-squared MM^{*2}, recoiling against the photon and the D_s^- tag should peak at the D_s^+ mass-squared.

The MM^{*2} distributions for events in the D_s^- invariant mass signal region ($\pm$17.5 MeV from the D_s mass) are shown in Fig. 2(b). In order to find the number of tags used for further analysis we perform a two-dimensional binned maximum liklihood fit of the MM^{*2} distribution and the invariant mass distribution in the interval $\pm$60 MeV from the D_s mass and $3.50 < \mathrm{MM}^{*2} < 4.25$ GeV^2. The background has two components, both described by 5th order Chebyshev polynomials; the first comes from the background under the invariant mass peak, defined by

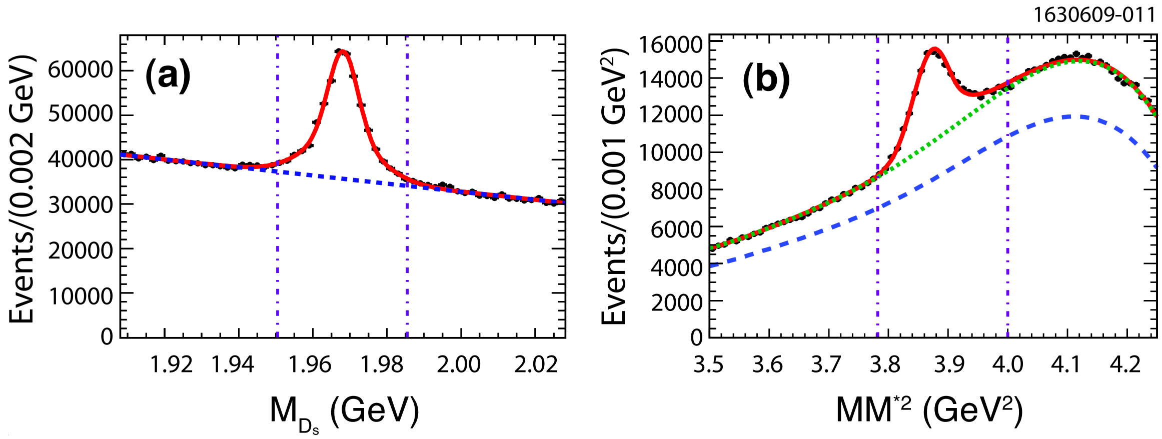

Figure 2: (a) Invariant mass of D_s^- candidates summed over the decay modes: $K^+K^-\pi^-$, K_sK^-, $\eta\pi^-$, $\eta'\pi^-$, $K^+K^-\pi^-\pi^0$, $\pi^+\pi^-\pi^-$, $K^{*-}K^{*0}$, $\eta\rho^-$, and fit to a two-Gaussian signal shape plus a linear background. No MM^{*2} cut has been applied. (b) The MM^{*2} distribution. The curves show a Crystal Ball function for signal and two 5th order Chebyshev background functions; the dashed curve shows the background from fake D_s^- tags, while the dotted curve in (b) shows the sum of the backgrounds from multiple photon combinations and fake D_s^- tags. The vertical dashed lines in (a) and (b) show the region of events selected for further analysis.

the sidebands, and the second is due to multiple photon combinations. In both cases we allow the parameters to float. We find a total of 43859±936±877 signal events in the interval $3.782 < \mathrm{MM}^{*2} < 4.000$ GeV^2 and having an invariant mass within ±17.5 MeV of the D_s mass.

With these tag samples CLEO measured the $D_s^+ \to \mu^+\nu$ and $\tau^+\nu$ final states with $\tau^+ \to \pi^+\nu$ and $\rho^+\nu$. The $\tau^+ \to e^+\nu\bar{\nu}$ was measured using a sub-set of invariant mass tags only. Here the sum of all of the energy deposited in the electromagnetic calorimeter, E_{extra}, that is not associated with either the tag or the τ^+ decay is used as an additional discriminant; for signal events E_{extra} should be zero.

The $\tau^+ \to \rho^+\nu$ analysis is quite novel. Here some backgrounds peak while the signal shape, that is extremely well known, is rather flat. E_{extra} is also used in this analysis. The MM^2 distribution computed from a D_s^- tag, a photon and a ρ^+ is shown on Fig. 3. A clear excess of signal events is present. A summary of measurements of $f_{D_s^+}$ by several groups are listed in Table 1.[1]

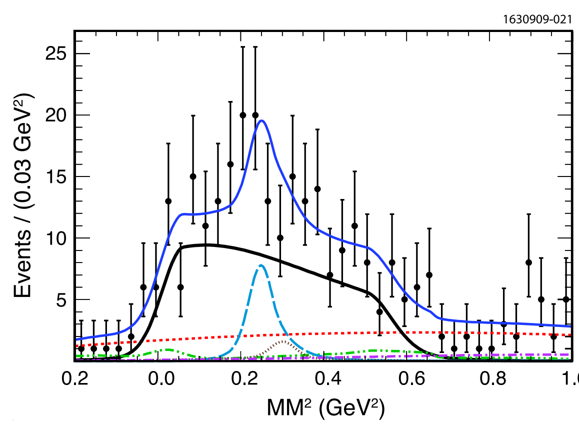

Figure 3: Fit to the data (points) for $E_{\mathrm{extra}} < 0.1$ GeV. The various components are signal (thick solid line), $\eta\rho^+$ (dotted), fake D_s^- (dashed), $K^0\pi^+\pi^0$ (long dash), sum of $\pi^+\pi^0\pi^0$, $\eta\pi^+$, $\phi\pi^+$, $\tau^+ \to (\pi^+ + \pi^+\pi^0\pi^0)\overline{\nu}$, $\mu^+\nu$, and $X\mu^+\nu$ (dash-dot-dot), and other backgrounds (dashed-dot). The thinner solid curve shows the total.

The decay constant average for $f_{D_s^+}$ is (257.5 ± 6.1) MeV. Two unquenched lattice QCD calculations using 3 light fermion loops (unquenched) are available.[7] HPQCD now quotes a value of (247±2) MeV, a 2σ change from their published value of (241±3) MeV. The updated Fermilab/MILC result is (261.4±7.7±5.0 MeV). They also predict $f_{D_+} = 220.3 \pm 8.0 \pm 4.3)$ MeV. Thus these preliminary theoretical results are in agreement with the data.

3 Semileptonic Decays

CLEO has observed $D_s^+ \to f_0(980)e^+\nu$; $f_0 \to \pi^+\pi^-$, measured the form-factor as a function of q^2, and determined the mass and width of the f_0, parameters that are not well known.[8] The rate

Table 1: Experimental results for $\mathcal{B}(D_s^+ \to \mu^+\nu)$, $\mathcal{B}(D_s^+ \to \tau^+\nu)$, and $f_{D_s^+}$.

Experiment	Mode	$\mathcal{B}$	$f_{D_s^+}$ (MeV)
CLEO-c [2]	$\mu^+\nu$	$(5.65 \pm 0.45 \pm 0.17) \times 10^{-3}$	$257.6 \pm 10.3 \pm 4.3$
Belle [3]	$\mu^+\nu$	$(6.38 \pm 0.76 \pm 0.57) \times 10^{-3}$	$274 \pm 16 \pm 12$
Average	$\mu^+\nu$	$(5.80 \pm 0.43) \times 10^{-3}$	261.5 ± 9.7
CLEO-c [2]	$\tau^+\nu\ (\pi^+\overline{\nu})$	$(6.42 \pm 0.81 \pm 0.18) \times 10^{-2}$	$278.0 \pm 17.5 \pm 3.8$
CLEO-c [4]	$\tau^+\nu\ (\rho^+\overline{\nu})$	$(5.52 \pm 0.57 \pm 0.21) \times 10^{-2}$	$257.8 \pm 13.3 \pm 5.2$
CLEO-c [5]	$\tau^+\nu\ (e^+\nu\overline{\nu})$	$(5.30 \pm 0.47 \pm 0.22) \times 10^{-2}$	$252.6 \pm 11.2 \pm 5.6$
BaBar [6]	$\tau^+\nu\ (e^+\nu\overline{\nu})$	$(4.54 \pm 0.53 \pm 0.40 \pm 0.28) \times 10^{-2}$	$233.8 \pm 13.7 \pm 12.6$
Average	$\tau^+\nu$	$(5.58 \pm 0.35) \times 10^{-2}$	255.5 ± 7.5
Average	$\mu^+\nu + \tau^+\nu$		257.5 ± 6.1

and form-factor for $D_s^+ \to \phi e^+\nu$ was also measured. The ratio of these two rates at q^2 of zero was predicted [9] to be similar to that of $\Gamma\left(B_s \to J/\psi f_0\right)/\Gamma\left(B_s \to J/\psi \phi\right)$.

Figure 4 shows the q^2 distributions. The $\phi e^+\nu$ channel is fit using the form factors determined by the BaBar collaboration letting the normalization float.[10] For $f_0 e^+\nu$ a simple pole model is used: $|f_+(q^2)| = 1/(1 - q^2/M^2_{\rm pole})$, resulting in $M_{\rm pole}$=$(1.7^{+4.5}_{-0.7}\pm 0.2)$ GeV. Using the fits we find that at q^2 of zero the f_0/ϕ yield is (42±011)%.

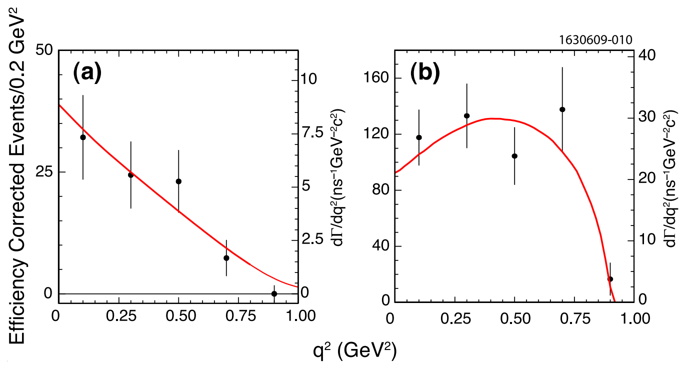

Figure 4: The q^2 distributions for (a) $D_s^+ \to f_0 e^+\nu$ (b) $D_s^+ \to \phi e^+\nu$. The fits are described in the text.

Acknowledgments

I thank the U. S. National Science Foundation for Support. I thank my CLEO colleagues especially M. Artuso, J. Rosner and L. Zhang. I apologize for the large amount of omitted material.

References

1. J. L. Rosner and S. Stone arXiv:1002.1655v2 [hep-ex].
2. J. P. Alexander *et al.*, (CLEO Collab.), *Phys. Rev.* D**79**, 052001 (2009); M. Artuso *et al.*, (CLEO Collab.), *Phys. Rev. Lett.* **99**, 071802 (2007).
3. L. Widhalm *et al.*, (Belle Collab.), *Phys. Rev. Lett.* **100**, 241801 (2008).
4. P. Naik *et al.*, (CLEO Collab.), *Phys. Rev.* D**80**, 112004 (2009).
5. P.U.E. Onyisi *et al.*, (CLEO Collab.), *Phys. Rev.* D**79**, 052002 (2009); K.M. Ecklund *et al.*, (CLEO Collab.), *Phys. Rev. Lett.* **100**, 161801 (2008).
6. J. Dingfelder, "Hot topics from Babar: Leptonic and Semileptonic *B* and *D* decays," presented at Moriond QCD and High Energy Interactions, La Thuile, Italy March 2010; J. P. Lee *et al.*, (BaBar Collab.) [arXiv:1003.3063].
7. C. Bernard, "Leptonic *B* and *D* Decays on the Lattice," Lattice QCD Meets Exp. Workshop, Ferimlab, April, 2010.
8. K. M. Ecklund *et al.*, (CLEO Collab.), *Phys. Rev.* D**80**, 052009 (2009); J. Yelton, *et al.*, (CLEO Collab.), *Phys. Rev.* D**80**, 052007 (2009).
9. S. Stone and L. Zhang, *Phys. Rev.* D**79**, 074024 (2009).
10. B. Aubert *et al.* (BaBar Collab.), *Phys. Rev.* D**78**, 051101 (2008).